

## Vortex Glass Transition in a Frustrated 3D XY Model with Disorder

Peter Olsson

*Department of Physics, Umeå University, 901 87 Umeå, Sweden*  
(Received 31 January 2003; published 12 August 2003)

The anisotropic frustrated three-dimensional (3D) XY model with disorder in the coupling constants is simulated as a model of a point disordered superconductor in an applied magnetic field. A finite size scaling analysis of the helicity modulus gives strong evidence for a finite temperature transition with isotropic scaling and the correlation length exponent  $\nu = 1.5 \pm 0.3$ , consistent with 3D gauge glass universality.

DOI: 10.1103/PhysRevLett.91.077002

PACS numbers: 74.25.Dw, 64.60.-i, 74.25.Qt

The hypothesis of a vortex glass in disordered high temperature superconductors [1,2] has spurred much research and many discussions during more than one decade and continues to be a very controversial issue [3]. The essence of this suggestion is that random point disorder in superconductors may conspire with the vortex line interaction to pin the vortices and that this takes place through a true thermodynamic phase transition into a phase with vanishing linear resistance.

Computer simulations have become an increasingly important tool for examining critical phenomena and have also recently been used in the study of some vortex glass models. One important such model is the three-dimensional (3D) gauge glass, which is an isotropic 3D XY model with randomness included through a random vector potential added to the phase difference of the superconducting order parameter. The evidence has for quite some time pointed at a finite temperature transition in this model [4,5], but strong evidence for a real phase transition has been obtained only recently [6] through the use of the exchange Monte Carlo (MC) technique [7]. The value of the correlation length exponent was then found to be  $\nu = 1.39 \pm 0.20$ . It is, however, generally recognized that the 3D gauge glass model is too much of a simplification to allow for any safe conclusions regarding the behavior of disordered superconductors in applied magnetic fields [4]. Most seriously, the gauge glass is an isotropic model with no net field, which means that the possibility of anisotropic scaling is excluded at the outset.

A few studies with the necessary ingredients of disorder and applied field have thus far been reported in the literature [8]. An examination of the frustrated 3D XY model with randomness in the couplings gave data that was interpreted as evidence for a phase transition with  $\nu \approx 2.2$  [9]. The crossing of the data for different sizes expected from finite size scaling, was, however, not entirely convincing, possibly because of the open boundary conditions employed in the simulation. By instead using periodic boundary conditions, the same author very recently obtained  $\nu \approx 1.1$  [10]; the crossings were, however, still not entirely satisfactory. Another study gives results for a 3D random pinning model with strong dis-

order [11]. The value of the correlation length exponent was there found to be  $\nu \approx 0.7$ , indistinguishable from  $\nu \approx 0.67$  in the pure zero-field 3D XY model. This is at odds with the common expectation that a vortex glass transition should be in a different universality class than the pure model. Finally, a very recent simulation study of a model which extends the elastic description of a vortex lattice to include dislocations gives a transition with  $\nu \approx 1.3$  [12].

In this Letter, we present results from large scale simulations on a frustrated 3D XY model with disorder in the coupling constants. The quantity in focus is the helicity modulus, and we find a finite temperature glass transition with isotropic scaling and the correlation length exponent  $\nu = 1.5 \pm 0.3$ . The agreement with  $\nu = 1.39 \pm 0.20$  for the 3D gauge glass model [6] suggests a common universality class.

The model we simulate is given by the Hamiltonian [13]

$$\mathcal{H} = - \sum_{\text{bonds } i\mu} J_{i\mu} \cos(\theta_i - \theta_{i+\hat{\mu}} - A_{i\mu} + \delta_{\mu}^{(\mathbf{r}_i, \hat{\mu})}), \quad (1)$$

where  $\theta_i$  is the phase of the superconducting wave function at site  $i$  with position  $\mathbf{r}_i$  of a periodic  $L_x \times L_y \times L_z$  lattice, and the sum is over all bonds in directions  $\mu = x, y, z$ . An applied magnetic field in the  $z$  direction corresponding to  $1/5$  flux quantum per plaquette is obtained through the quenched vector potential with the choice  $A_{ix} = y_i 2\pi/5$ , and  $A_{iy} = A_{iz} = 0$ . The randomness is included through disorder in the coupling constants,

$$\begin{aligned} J_{i\mu} &= J_{\perp}(1 + p\epsilon_{i\mu}), & \mu &= x, y, \\ J_{i\mu} &= J_{\parallel}, & \mu &= z, \end{aligned}$$

where  $\epsilon_{i\mu}$  are independent variables from a Gaussian distribution with  $\langle \epsilon_{i\mu} \rangle = 0$  and  $\langle \epsilon_{i\mu}^2 \rangle = 1$ . The disorder strength and the anisotropy were chosen as  $p = 0.4$  and  $J_{\parallel} = J_{\perp}/40$ . The simulations are performed with fluctuating twist boundary conditions [14] which in the duality relation corresponds to a vortex line model with periodic boundary conditions. We make use of  $L_{\mu}$  twist variables  $\delta_{\mu}^{(\mathbf{r}_i, \hat{\mu})}$  for each direction and the total twist in

the respective directions is  $\Delta_\mu = \sum_{j=1}^{L_\mu} \delta_\mu^{(j)}$ . Standard Metropolis steps are used both for the angular variables and for updating the twist variables  $\delta_\mu^{(r;\hat{\mu})}$ . The simulations are performed with  $L = L_x = L_y$  and most of them with a fixed aspect ratio,  $L/L_z = 5/3$ . The temperature is given in units of  $J_\perp$ .

A short comment on the choice of the parameters: The anisotropy  $J_\perp/J_\parallel = 40$  was chosen to allow for enough fluctuations in the field direction and to avoid the formation of Abrikosov lattices. (This was checked by examining the in-plane vortex structure factor [13].) Since general theoretical considerations [2] give at hand that the correlation length along  $z$  is  $\propto \sqrt{J_\parallel/J_\perp}$ , this anisotropy together with the aspect ratio  $L_z/L = 3/5$  would correspond to an isotropic model with  $L_z/L \approx 3.8$ .

The quantity in focus in our analysis is the helicity modulus which is defined from the change in free energy density,  $f$ , due to an applied twist,  $\delta_\mu$ :  $Y_\mu = \partial^2 f / \partial \delta_\mu^2$  [15]. To use the helicity modulus as a signal of the stiffness of the system, the derivative should be evaluated at the twist that minimizes the free energy. In nonrandom systems, this minimum is always at zero twist and the helicity modulus may then be evaluated by means of a correlation function determined with periodic boundary conditions,  $\Delta_\mu = 0$ . For disordered systems, however, the minimizing twist will in general be different from zero and one then needs to make simulations with the twist variables  $\Delta_\mu$  as additional dynamical variables and collect histograms  $P_\mu(\Delta_\mu)$ . The helicity moduli are then determined from the free energies  $F_\mu = -T \ln P_\mu$ , as discussed below. To analyze the critical behavior, we use the standard scaling relation for the helicity modulus in 3D,

$$LY \sim g(tL^{1/\nu}), \quad (2)$$

where  $t = (T - T_c)/T_c$  and  $g$  is a scaling function [16]. In Ref. [13], a naive analysis of  $Y(L)$  rather than the correct scaling quantity  $LY$  led to the erroneous conclusion of no vortex glass phase in this model. Equation (2) presumes isotropic scaling,  $\zeta = 1$ . In the general case, the system sizes should be chosen with  $L_z \propto L^\zeta$  and the scaling quantities are then  $L^\zeta Y_\perp$  and  $L^{2-\zeta} Y_\parallel$ , respectively [11].

Our simulations are performed with the exchange MC technique, which is a method for simultaneously simulating multiple copies of a particular configuration of disorder with each copy at a different temperature. According to certain rules, these copies may now and then interchange temperature [7] and therefore effectively perform random walks in temperature space which greatly help the different copies avoid getting trapped in restricted parts of the phase space. This makes it possible to sample the whole phase space and obtain the true thermodynamic averages. In our simulations the temperatures were chosen according to the equation

$$T_m = T_{\min} \left( \frac{T_{\max}}{T_{\min}} \right)^{m/N_T}, \quad m = 0, \dots, N_T - 1, \quad (3)$$

with  $T_{\max} = 0.24$  and  $T_{\min}$  as given in Table I. Before doing the actual exchange MC simulations, the initial spin configurations for the  $N_T$  temperatures were obtained by slowly cooling the system with standard MC simulations. The number of temperatures, the acceptance ratio for the exchange step, and the number of disorders simulated for the different system sizes are shown in Table I. The exchange steps are attempted once every 16 sweeps.

The exchange MC method ensures that all the different copies remain at thermal equilibrium as soon as equilibrium has been reached. The approach to equilibrium may however be very slow. We have carefully examined the approach to equilibrium and, especially for our largest sizes, the times for equilibration are indeed very long. For the next largest size,  $L = 20$ , equilibration is only reached after about  $2.9 \times 10^6$  sweeps, and to make thermalization at all possible for our largest size,  $L = 25$ , we chose not to go to quite that low temperature for the largest size, cf. Table I. This was decided since the time required for thermalization may increase very rapidly with decreasing temperature. Still, about  $4.5 \times 10^6$  sweeps were necessary to reach equilibrium for  $L = 25$ .

For each system size, disorder configuration, and temperature, the main output from the simulations is histograms  $P_\mu(\Delta_\mu; \tau)$ , where  $\tau$  enumerates bins corresponding to  $2^{18} = 262\,144$  sweeps over the lattice. The further analysis is then based on averages such as

$$\bar{P}_\mu(\Delta_\mu) = \frac{1}{\tau_{\max}} \sum_{\tau=1}^{\tau_{\max}} P_\mu(\Delta_\mu; \tau),$$

(see Fig. 1) and the helicity modulus is determined from the curvature at the minimum of the associated free energy by fitting a second order polynomial to the free energy in a narrow interval around the minimum,  $\Delta_\mu^0$ , which is also determined in the fit,

$$\bar{F}_\mu(\Delta_\mu) \sim Y_\mu(V/2L_\mu^2)(\Delta_\mu - \Delta_\mu^0)^2. \quad (4)$$

With  $[\dots]_{\text{av}}$  denoting the average over disorder configurations, we define

TABLE I. Parameters describing the simulations. For systems of size  $L \times L \times L_z$ , we simulated  $N_d$  disorder configurations with  $N_T$  temperatures in the range  $T_{\min} \leq T < T_{\max}$ , cf. Eq. (3). The acceptance ratio for the exchange step is given by  $X_{\text{acc}}$ . Of the bins corresponding to  $2^{18} = 262\,144$  sweeps,  $\tau_{\text{eq}}$  are first discarded and the remaining  $\tau_{\text{max}}$  are used for calculating averages. The same information is also given in terms of the number of sweeps for equilibration and for collecting data.

$L$	$L_z$	$N_d$	$N_T$	$T_{\min}$	$X_{\text{acc}}$ (%)	$\tau_{\text{eq}}$	$\tau_{\text{max}}$	Sweeps/ $10^6$
10	6	600	12	0.09	30	1	15	0.3 + 3.9
15	9	600	24	0.09	30	4	12	1.0 + 3.1
20	12	600	36	0.09	32	11	21	2.9 + 5.5
25	15	200	36	0.115	27	17	31	4.5 + 8.1

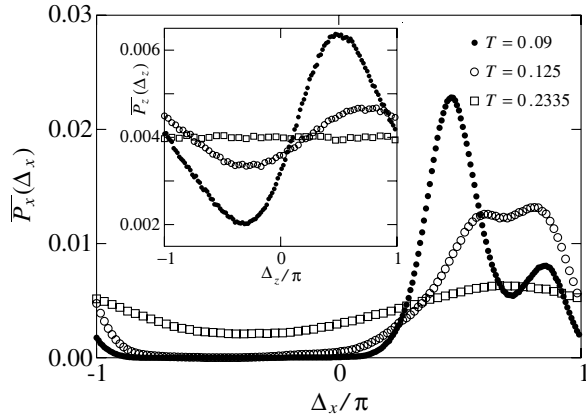


FIG. 1.  $\bar{P}_x(\Delta_x)$  for a certain disorder realization. Note that the peaks of the histograms become higher and sharper as the temperature is lowered. This kind of data is used for the determination of  $Y_x$  through Eq. (4). The inset gives the corresponding quantity for the  $z$  direction.

$$Y_{\perp} = \frac{1}{2}[Y_x + Y_y]_{\text{av}}, \quad (5a)$$

$$Y_{\parallel} = [Y_z]_{\text{av}}. \quad (5b)$$

It turns out that the values of the helicity moduli obtained with the above equations are biased towards too large values. To investigate the reason for this bias, we performed additional simulations with fluctuating twist boundary conditions of the pure zero-field 3D  $XY$  model and collected histograms  $P(\Delta, \tau)$ , where  $\tau$  enumerates the bins. This data was then used to calculate averages over  $\tau_{\text{aver}}$  consecutive bins  $\bar{P}(\Delta; \tau_{\text{aver}})$ . These histograms for different run lengths were then used to determine  $Y$ , and from the dependence of  $Y$  on  $\tau_{\text{aver}}$  it was found that the bias decays as  $1/\tau_{\text{aver}}$  to a very good precision. It was also found that the bias may be made to vanish altogether by making use of  $\Delta^0 = 0$  in Eq. (4) instead of using  $\Delta^0$  as a free parameter. ( $\Delta^0 = 0$  is the known value of the minimizing twist in the pure system.) This observation suggests that the bias is related to the usual complication in determining the width (variance) of a distribution when the true average is not known [17]. Since  $Y$  is inversely related to the variance of  $P(\Delta)$  around the maximum, it follows that the estimates based on runs of length  $\tau_{\text{aver}}$  would be expected to decay towards the true value as [17]

$$Y(\tau_{\text{aver}}) = Y(\infty)/(1 - b/\tau_{\text{aver}}), \quad (6)$$

where  $b$  is a free parameter related to the decorrelation time in the simulations. For small values of  $b/\tau_{\text{aver}}$ , this is in accordance with the  $1/\tau_{\text{aver}}$  decay discussed above.

Returning to the vortex glass model, the procedure used to determine our final data consists of three steps: (i) Determine  $Y_{\mu}(\tau_{\text{aver}})$  for each disorder configuration and several values of  $\tau_{\text{aver}}$  by fitting histogram  $\bar{P}_{\mu}(\Delta_{\mu}; \tau_{\text{aver}})$  based on  $\tau_{\text{aver}}$  consecutive bins,  $P_{\mu}(\Delta_{\mu}, \tau)$  to Eq. (4). (ii) Calculate the disorder averaged quantities  $Y_{\perp}(\tau_{\text{aver}})$  and  $Y_{\parallel}(\tau_{\text{aver}})$  cf. Eqs. (5). (iii) Fit this data to

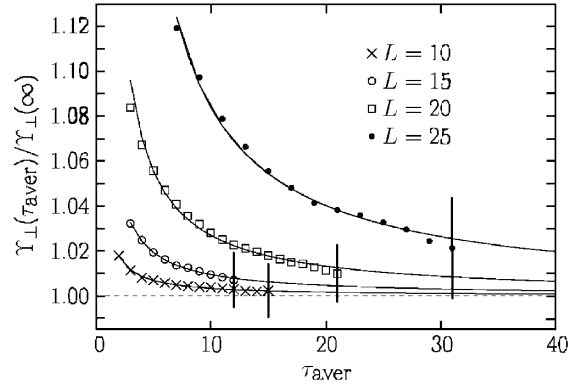


FIG. 2. The figure shows the elimination of the bias in  $Y_{\perp}$  by fitting  $Y_{\perp}(\tau_{\text{aver}})$  to Eq. (6) with  $b$  and  $Y_{\perp}(\infty)$  as free parameters. The solid lines are  $1/(1 - b/\tau_{\text{aver}})$ . The time is in units of the bin size,  $2^{18}$  sweeps.

Eq. (6) to obtain the unbiased estimates  $Y_{\perp} \equiv Y_{\perp}(\infty)$  and  $Y_{\parallel} \equiv Y_{\parallel}(\infty)$ . The last step is illustrated in Fig. 2 for  $T = 0.125$  close to  $T_c$ . The error bars on the last points are the errors associated with the disorder averages.

We first assume isotropic scaling and plot  $LY_{\perp}$  for systems with fixed aspect ratio in Fig. 3. To a very good accuracy, the data for the different sizes cross at a single temperature. To further verify the scaling according to Eq. (2), we fit our data for  $LY_{\perp}$  near  $T_c$  to a fourth order polynomial expansion of  $g(tL^{1/\nu})$  and obtain the values  $\nu = 1.5 \pm 0.3$  and  $T_c = 0.123 \pm 0.008$ . The collapse which is shown in Fig. 4 is excellent and holds in a surprisingly large temperature interval.

A vortex glass transition should also be seen in the parallel component of the helicity modulus. The crossing of  $LY_{\parallel}$  for different sizes at  $T_c$  and the scaling collapse are shown in the insets of Figs. 3 and 4, respectively. From the not so smooth curves, it is clear that the precision in  $Y_{\parallel}$  is much worse than for  $Y_{\perp}$ . This may be traced back to the less good quality of the histograms  $\bar{P}_z(\Delta_z)$ , as shown

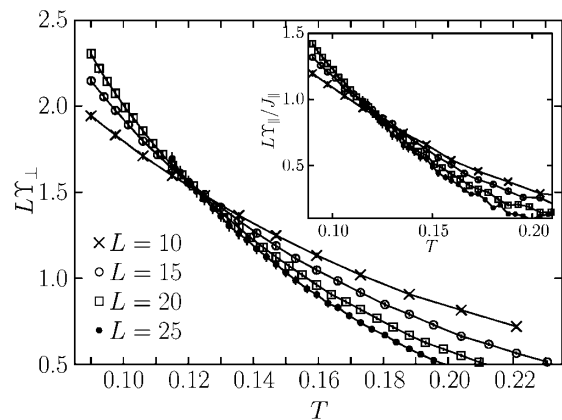


FIG. 3.  $LY_{\perp}$  versus temperature for four different system sizes. The curves cross at a single point, which is an indication of critical behavior. The inset shows  $LY_{\parallel}/J_{\parallel}$  which shows a similar crossing at almost the same temperature.

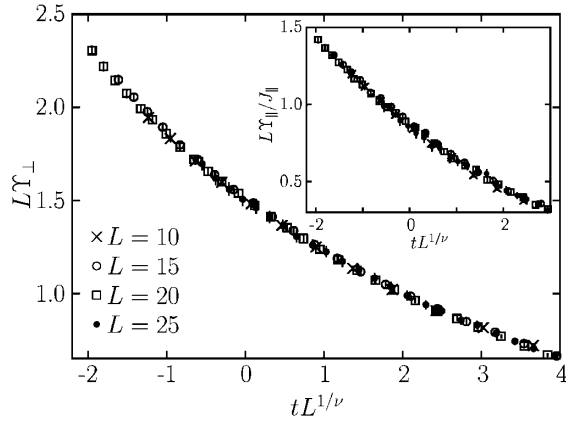


FIG. 4. The scaling collapse of  $LY_{\perp}$  gives  $\nu = 1.5 \pm 0.3$  and  $T_c = 0.123 \pm 0.008$ . The inset is a collapse of  $LY_{\parallel}/J_{\parallel}$  with the same values for  $\nu$  and  $T_c$ .

in the inset of Fig. 1. Nevertheless, the data for  $LY_{\parallel}$  (see inset of Fig. 4) collapse nicely when using the same values of  $\nu$  and  $T_c$  as in the main figure.

To check for the possibility that our data could also be collapsed with the anisotropy exponent  $\zeta \neq 1$ , we have performed some additional simulations with different aspect ratios,  $L_z = 5, 7$  for  $L = 10$  and  $L_z = 8, 10$  for  $L = 15$ , and attempted finite size scaling analyses with  $L_z \propto L^{\zeta}$  for  $L = 10, 15$ , and  $20$ . It is then found that the attempted collapse of  $L^{\zeta}Y_{\perp}$  rapidly becomes worse when  $\zeta$  is changed from unity, but the clearest signal for the breakdown of scaling comes from examining the tentative crossing temperatures for  $L^{\zeta}Y_{\perp}$  and  $L^{2-\zeta}Y_{\parallel}$ , respectively. These crossing temperatures are the same for  $\zeta = 1$ , cf. Fig. 3, but it is found that they move in the opposite directions when  $\zeta$  is changed away from unity. This is a very sensitive test which gives  $0.9 < \zeta < 1.1$ .

We now shortly discuss the relation between the helicity modulus calculated in the present paper and the more common method to determine the root mean square current,  $I_{\text{rms}}$  [5]. Since the current and the helicity modulus are first and second derivatives, respectively, of the same function  $F(\Delta)$ , both quantities effectively probe the roughness of this function. The low temperature phase is characterized by large energy barriers growing with system size, whereas  $F(\Delta)$  above the transition temperature becomes a flat function in the limit of large  $L$ . However,  $Y$  turns out to be more efficient in measuring the roughness of  $F(\Delta)$ . The reason is that  $Y$  measures a property at an extremum (the minimum of the free energy), whereas the current at  $\Delta = 0$  for a given shape of the function may be large or small depending on the location of the structure in  $F(\Delta)$ .  $I_{\text{rms}}$  is therefore only *on the average* a good measure of the properties of  $F(\Delta)$  and this has to be compensated for by using a larger number of disorder configurations. This is the reason for the good precision in our data in spite of the rather small number of disorder configurations.

Note also that there is a bias in the determination of  $I_{\text{rms}}$  that is very similar to the bias in  $Y$  discussed above. For  $I_{\text{rms}} = \sqrt{[I^2]_{\text{av}}}$ , the origin of this bias is that the statistical error  $\delta I$  gives a term  $(\delta I)^2 \geq 0$ . Since  $\delta I$  should vanish with simulation time as  $\sim 1/\sqrt{\tau_{\text{aver}}}$ , the bias in  $I_{\text{rms}}$  would vanish as  $1/\tau_{\text{aver}}$ , which is essentially the same as the behavior of  $Y(\tau_{\text{aver}})$ . There is, however, a difference in that the bias in  $I_{\text{rms}}$  is easily eliminated by performing two independent simulations,  $\alpha$  and  $\beta$ , for each disorder and measuring the quantity  $[I_{\alpha}I_{\beta}]_{\text{av}}$  [6]. The bias in  $Y$  cannot be eliminated with such methods.

In summary, we have performed a finite size scaling analysis of the helicity modulus in a frustrated 3D  $XY$  model with disorder. We find isotropic scaling with  $\nu = 1.5 \pm 0.3$ . The good agreement with  $\nu = 1.39 \pm 0.20$  of the 3D gauge glass suggests that the two models actually do belong to same universality class.

The author would like to acknowledge helpful discussions with S. Teitel and M. Wallin. This work has been supported by the Swedish Research Council, Contract No. E 5106-1643/1999, and by the resources of the Swedish High Performance Computing Center North (HPC2N).

- 
- [1] M. P. A. Fisher, Phys. Rev. Lett. **62**, 1415 (1989).
  - [2] D. S. Fisher, M. P. A. Fisher, and D. A. Huse, Phys. Rev. B **43**, 130 (1991).
  - [3] C. Reichhardt, A. van Otterlo, and G. T. Zimányi, Phys. Rev. Lett. **84**, 1994 (2000).
  - [4] D. A. Huse and H. S. Seung, Phys. Rev. B **42**, 1059 (1990).
  - [5] J. D. Reger, T. A. Tokuyasu, A. P. Young, and M. P. A. Fisher, Phys. Rev. B **44**, 7147 (1991).
  - [6] T. Olson and A. P. Young, Phys. Rev. B **61**, 12 467 (2000).
  - [7] K. Hukushima and K. Nemoto, J. Phys. Soc. Jpn. **65**, 1604 (1996).
  - [8] M. J. P. Gingras, Phys. Rev. B **45**, 7547 (1992).
  - [9] H. Kawamura, J. Phys. Soc. Jpn. **69**, 29 (2000).
  - [10] H. Kawamura, cond-mat/0302284, completed after the submission of this paper.
  - [11] A. Vestergren, J. Lidmar, and M. Wallin, Phys. Rev. Lett. **88**, 117004 (2002).
  - [12] J. Lidmar, cond-mat/0302577.
  - [13] P. Olsson and S. Teitel, Phys. Rev. Lett. **87**, 137001 (2001).
  - [14] P. Olsson, Phys. Rev. B **52**, 4511 (1995).
  - [15] M. E. Fisher, M. N. Barber, and D. Jasnow, Phys. Rev. A **8**, 1111 (1973).
  - [16] Y.-H. Li and S. Teitel, Phys. Rev. B **40**, 9122 (1989).
  - [17] To get an unbiased estimate of the variance of a distribution based on  $N$  independent values  $x_i$ , one should make use of  $\sigma^2 = 1/(N-1) \sum (x_i - \bar{x})^2$ . The prefactor here differs from the naively expected  $1/N$  since the value of the average  $\bar{x}$  in general is different from the true average of the distribution. The connection with Eq. (6) follows since this may be written  $\sigma_{\text{naive}}^2(N) = (1 - 1/N)\sigma^2$ .